



Louse flies holding on mammals' hair: Comparative functional morphology of specialized attachment devices of ectoparasites (Diptera: Hippoboscoidea)

Sarah Hayer  | Beeke P. Sturm | Sebastian Büsse  | Thies H. Büscher | Stanislav N. Gorb

Department of Functional Morphology and Biomechanics, Zoological Institute, Kiel University, Kiel, Germany

Correspondence

Sarah Hayer, Department of Functional Morphology and Biomechanics, Zoological Institute, Kiel University, Am Botanischen Garten 1–9, 24098 Kiel, Germany.
Email: shayer@zoologie.uni-kiel.de and sarah.hayer@gmx.de

Abstract

Hippoboscidae and Nycteribiidae of the dipteran superfamily Hippoboscoidea are obligate ectoparasites, which feed on the blood of different mammals. Due to their limited flight capability, the attachment system on all tarsi is of great importance for a secure grasp onto their host and thus for their survival. In this study, the functional morphology of the attachment system of two hippoboscid species and two nycteribiid species was compared in their specificity to the host substrate. Based on data from scanning electron microscopy and confocal laser scanning microscopy, it was shown that the attachment systems of both Hippoboscidae and Nycteribiidae (Hippoboscoidea) differ greatly from that of other calyptrate flies and are uniform within the respective families. All studied species have an attachment system with two monodentate claws and two pulvilli. The claws and pulvilli of the Hippoboscidae are asymmetric, which is an adaptation to the fur of even-toed ungulates (Artiodactyla). The fur of these mammals possesses both, thinner woolen and thicker coat hair; thus, the asymmetry of the attachment system of the hippoboscid species enables a secure attachment to all surfaces of their hosts. The claws and pulvilli of the nycteribiid species do not show an asymmetry, since the fur of their bat (Chiroptera) hosts consists of hairs with the same thickness. The claws are important for the attachment to mammals' fur, because they enable a secure grip by mechanical interlocking of the hairs through the claws. Additionally, well-developed pulvilli are able to attach on thicker hairs of Artiodactyla or on smooth substrates such as the skin.

KEYWORDS

adhesion, biomechanics, ecomorphology, friction, interlocking

This is an open access article under the terms of the Creative Commons Attribution-NonCommercial License, which permits use, distribution and reproduction in any medium, provided the original work is properly cited and is not used for commercial purposes.

© 2022 The Authors. *Journal of Morphology* published by Wiley Periodicals LLC.

1 | INTRODUCTION

Hippoboscoidea comprises four ectoparasitic dipteran lineages—Hippoboscidae (louse flies), Nycteribiidae and Streblidae (ked and bat flies), and Glossinidae (tse tse flies). The Glossinidae are the only free-living ectoparasites, while the other three families are obligate ectoparasites. They can either be completely wingless (e.g., Nycteribiidae) or shed their wings after having found a suitable host (e.g., *Lipoptena cervi*) or can be able to fly throughout their life (e.g., *Hippobosca equina*; Bequaert, 1953; Lloyd, 2002; Whitaker, 1988). In representatives of Hippoboscidae, the wings are often shed as soon as a suitable host is found, and the parasites stay on the same host for the rest of their life (Bequaert, 1953). An exception to this rule is *H. equina* Linnaeus, 1758 that keeps its wings and is therefore not necessarily restricted to one host only (Bequaert, 1953).

Generally, the loss of the ability to fly is considered an evolutionary adaptation to the lifestyle as obligate parasites (Bequaert, 1953; Ter Hofstede et al., 2004), suggesting that the parasite is dependent on the host to complete its life cycle (L. S. Roberts & Janovy, 2000). Within the Hippoboscoidea, the Hippoboscidae are adapted to birds and mammals as hosts, except for bats, which are exclusively parasitized by Nycteribiidae and Streblidae (Bequaert, 1953; Lloyd, 2002). The host extension to bats is considered a key innovation in the evolution of Hippoboscoidea (E. T. Petersen et al., 2007). Obligate parasites, in general, gain three main advantages due to the tight attachment to the host throughout their life, because the hosts provide them with shelter, energy, and motility (Combes, 2001). However, due to the inability to fly, most Hippoboscoidea are at disadvantage should they lose their host, contrasted by the increased motility on the host itself (E. T. Petersen et al., 2007). Without wings, the motility to find a new host is limited and often necessitates hosts with rather close contact of several individuals and overlapping generations as in gregarious bats (Reckardt & Kerth, 2006). Therefore, a reliable attachment system is of paramount importance for the survival of many obligate parasites in general and the wingless flies from the superfamily Hippoboscoidea in particular (Marshall, 1981).

The attachment system of Hippoboscidae and Nycteribiidae has only been studied for a few species in detail so far, for example, the hippoboscidian species *Crataerina pallida* (Liu et al., 2019; D. S. Petersen et al., 2018). The attachment system of *C. pallida* is modified in several aspects, when comparing it to other flying flies. Commonly, attachment devices of brachyceran Diptera are composed of monodentate claws, adhesive pads or pulvilli and an empodium (Friedemann et al., 2014; S. Gorb & Beutel, 2001; Niederegger & Gorb, 2003). Attachment to the smooth substrates is ensured by the pulvilli, which are covered by many tenent setae that can make reliable contact to diverse substrates (S. Gorb & Beutel, 2001; Persson & Gorb, 2003). Claws support adhesion due to (1) their participation in the correct alignment of the pulvilli, (2) their help with detachment, and/or (3) mechanical interlocking with the substrates having coarser roughness (Dai et al., 2002; S. N. Gorb, 2001; Niederegger & Gorb, 2003). In contrast to this general dipteran

attachment system, *C. pallida* that is monoxenous for the common swift (*Apus apus*) has large tridentate claws and well-developed pulvilli (Kemper, 1951; Liu et al., 2019; Oldroyd, 1966; D. S. Petersen et al., 2018). Here, the claws are mainly responsible for attachment as they efficiently interlock with the feathers' vane. The dichotomously branching setae on the pulvilli are responsible for the attachment to smooth surfaces (D. S. Petersen et al., 2018). Both parts of the attachment system of *C. pallida* are evolutionary adapted to the bird host (D. S. Petersen et al., 2018). Preliminary studies have been undertaken for another hippoboscidian species, *L. cervi* (Linnaeus, 1758), which is adapted to the fur of deer, but can also be found on other large Artiodactyla (Bequaert, 1953; Haarløv & Haarlov, 1964; Kaitala et al., 2009). The claws and pulvilli on each tarsus are of different size, enabling to grasp both the woolen and coat hairs. Hairs with smaller diameter were observed to be clamped between claw tip and claw base, while larger hair was attached to the pulvillus (Haarløv & Haarlov, 1964). Generally, parasitic dipterans facilitate secure attachment to their different, often specific, hosts by fine tuning the claw morphology to the morphology of fur and feathers of the hosts supported by the pulvilli (Büscher et al., 2021; D. S. Petersen et al., 2018).

The aim of this study is to compare the functional morphology of the tarsal attachment systems of four different species of the two families Hippoboscidae and Nycteribiidae: the two hippoboscidian species *L. cervi* associated with deer and *H. equina* (Linnaeus, 1758) parasitizing cattle and horses. Both host species have heterogeneous fur composed of top coat and woolly hair underneath. Our aim is to investigate the specificity of the attachment system to the particular part of the host fur and to determine whether the attachment system is particularly adapted to either top coat or woolly hair. Interestingly, *L. cervi* sheds its wings after having found a host and *H. equina* keeps its wings throughout adulthood. Because of these differences in flight ability, the attachment system of both species is investigated comparatively to determine differences in the morphology of the attachment system. Furthermore, two nycteribiid species are compared to each other and to the above representatives of Hippoboscoidea: *Basilia nana* (Theodor & Moscona, 1954), which is monoxenous for the bat *Myotis bechsteini* and *Nycteribia kolenatii* (Theodor & Moscona, 1954) that is adapted to the bat *Myotis daubentoni*. Our aim is to identify species-specific differences in the attachment system in its adaptation to the specific host.

2 | MATERIAL & METHODS

2.1 | Species studied

Details of all four fly species studied can be found in Table 1. The species were collected between May and August in 2019 and preserved in 70% ethanol. Generally, two specimens of each species were used for scanning electron microscopy (SEM) and one specimen per species for confocal laser scanning microscopy (CLSM), respectively. The legs of each specimen were dissected and prepared for the respective method accordingly.

TABLE 1 Details of the fly species studied

Species	Family	Host	Sampling location
<i>Lipoptena cervi</i> (Linnaeus, 1758)	Hippoboscidae	<i>Capreolus capreolus</i> (roe deer) and <i>Cervus elaphus</i> (red deer)	Cesis, Latvia
<i>Hippobosca equina</i> (Linnaeus, 1758)	Hippoboscidae	mainly on <i>Equus</i> sp. (horses), but can maintain populations on cattle	Veterinary practice Seedorf, Germany
<i>Basilina nana</i> (Theodor & Moscona, 1954)	Nycteribiidae	<i>Myotis bechsteini</i> (Vespertilionidae)	NABU Osnabrück, Germany
<i>Nycteribia kolenatii</i> (Theodor & Moscona, 1954)	Nycteribiidae	<i>Myotis daubentoni</i> (Vespertilionidae)	NABU Osnabrück, Germany

Individual hairs of horses were obtained from the “Kieler Renn- und Reiterverein von 1902 e.V.” in May 2021, while the hairs of the bat *Myotis myotis* was obtained from the Zoological Museum Kiel and the fur of the deer were collected in Schleswig-Holstein by local hunters.

2.2 | Scanning electron microscopy

For scanning electron microscopy (SEM) analysis, the legs were dehydrated in an ascending ethanol series and critical-point dried using a Leica EM CPD300 (Leica). Both legs and hairs of vertebrates were sputter-coated with 10 μm of gold-palladium (Leica Bal-TEC SCD500; Leica Microsystems GmbH). Subsequently, the samples were mounted on a rotatable sample holder (Pohl, 2010) and examined using a Hitachi TM3000 scanning electron microscope (Hitachi Ltd Corporation). Only the pulvilli of the smaller species *L. cervi*, *B. nana*, and *N. kolenatii* were studied with a Hitachi S-4800 (Hitachi Ltd Corporation). Post-processing of the images was done with Adobe Photoshop CS6 (Adobe Inc.) and Affinity Photo (Serif Ltd) software.

2.3 | Confocal laser scanning microscopy

One specimen per species was used for confocal laser scanning microscopy (CLSM) analyses. The dissected legs were transferred to glycerine ($\geq 99.5\%$). Afterwards, samples were mounted on a glass slide using glycerine and covered with a high-precision glass coverslip. The autofluorescence signals of the samples' material compositions were examined using the CLSM Zeiss LSM700 (Carl Zeiss Micro Imaging GmbH) equipped with four stable solid-state lasers (cf. Michels & Gorb, 2012). The 405 nm laser line in combination with a bandpass emission filter transmitting 420–480 nm captured the autofluorescence of less sclerotized or resilin-dominated tissues. Longer wavelengths of 488 and 555 nm laser lines together with long-pass emission filters transmitting light wavelengths equal to or larger than 490 and 560 nm detected the autofluorescence of more sclerotized parts. Autofluorescence exceeding this range was captured with the 639 nm line in combination with the above-mentioned 560 nm long-pass emission filter (for wavelength and filter see Figure 1 in Büsse & Gorb, 2018). The

obtained autofluorescence was subsequently processed by maximum intensity projection using the software packages ZEN (Carl Zeiss MicroImaging GmbH) resulting in images illustrating less sclerotized, presumably soft materials in blue, more sclerotized (likely stiffer) materials in green, and strongly sclerotized parts in red. The graphics were edited using Affinity Photo (Serif Ltd) and Adobe Photoshop CS6 (Adobe Inc.).

2.4 | Morphometry of the attachment system

The length of all tarsomeres, claws, pulvilli with acanthae, and the empodium, where present, were measured. The measurements of all species were taken from the SEM pictures of two specimens and displayed in the Results with $n = 2$ (using Adobe Photoshop CS6 [Adobe Inc.] and Affinity Photo [Serif Ltd] software). For small structures, both legs of a pair of walking legs of two specimens were used, therefore resulting in four measurements ($n = 4$). The individual measurements are given in the Supporting Information (Table S1).

To quantify the density of acanthae on the pulvilli, a $10 \times 10 \mu\text{m}$ frame was applied on different areas of the SEM images using Adobe Photoshop CS6 (Adobe Inc.) and Affinity Photo (Serif Ltd) software. All acanthae within the frame were counted and the calculated mean value represents the density of acanthae per $100 \mu\text{m}^2$. According to Richards and Richards (1979) these protuberances on the pulvilli are called acanthae, since they do not show a socket.

3 | RESULTS

3.1 | General morphology of the attachment system

The attachment system of all four species consists of three parts: one pair of monodentate claws and a pair of pulvilli (fibrillar adhesive pads) located beneath the claws. The two species (*H. equina* and *L. cervi*) that are parasitizing larger mammals additionally have an empodium located between the two pulvilli, which is common in dipterans (Friedemann et al., 2014; S. Gorb & Beutel, 2001; Niederegger & Gorb, 2003). All claw segments differ in their width,

length, and shape, although similarities are found between the species of the same family. The largest attachment system is found in *H. equina*, *L. cervi*, and *N. kolenatii*, while *B. nana* has the smallest attachment system. No specific differences in the attachment system of the three leg pairs are revealed within either of the species.

3.2 | Surface morphology of the attachment system of Hippoboscid species

The tarsal attachment system of *H. equina* is asymmetrical, because the medial claw (mCL) is larger than the lateral claw (ICL; see Figure 1a). The larger mCL is $473 \pm 12 \mu\text{m}$ long (mean \pm SD, $n = 2$), the smaller claw is $325 \pm 10 \mu\text{m}$ long ($n = 2$), which is only 67.1% of the length of the mCL. Both claws emerge from a thick, stout base and taper at the end, while they bent proximally. The acute tips slightly bent toward the tarsi (Figure 1b). The tip of the larger mCL is $4.72 \pm 1.42 \mu\text{m}$ ($n = 2$) in diameter, while the smaller, ICL tip diameter is only $3.83 \pm 0.78 \mu\text{m}$ ($n = 2$). The bases from where the

claws originate are $315.3 \pm 2.0 \mu\text{m}$ ($n = 4$) and $226.6 \pm 2.4 \mu\text{m}$ ($n = 4$) long, respectively. Although the bases have a different total length, the proximal part making contact with the fifth tarsomere (T5) is of the same size (Figure 1a). Due to different claw sizes, the width of the gap between the claw base and the claw itself also differ slightly between the medial and ICLs. The widths measured proximally on the claw base are $21 \pm 2.74 \mu\text{m}$ ($n = 4$) for the mCL and $27 \pm 1.22 \mu\text{m}$ ($n = 4$) for the ICL. The gap is widest between the distal end of the claw base and the opposing claw, resulting in $39.25 \pm 6.38 \mu\text{m}$ ($n = 4$) for the mCL and $53.5 \pm 4.33 \mu\text{m}$ ($n = 4$) for the smaller, ICL. This difference in the measured gap width displays that the larger, mCL is bent more toward the claw base than the smaller lateral one.

On the bases of both claws, as well as on the claws themselves, prominent grooves are visible (Figure 1a–c). The grooves on the claw bases are found on the distal edge opposite the claws, which run diagonally from the medial-ventral to the lateral-dorsal side (Figure 1a). On the claws themselves, the grooves are present from the proximal-dorsal edge toward the proximal-ventral tip on both the medial and the lateral sides of the claw, running diagonally toward the

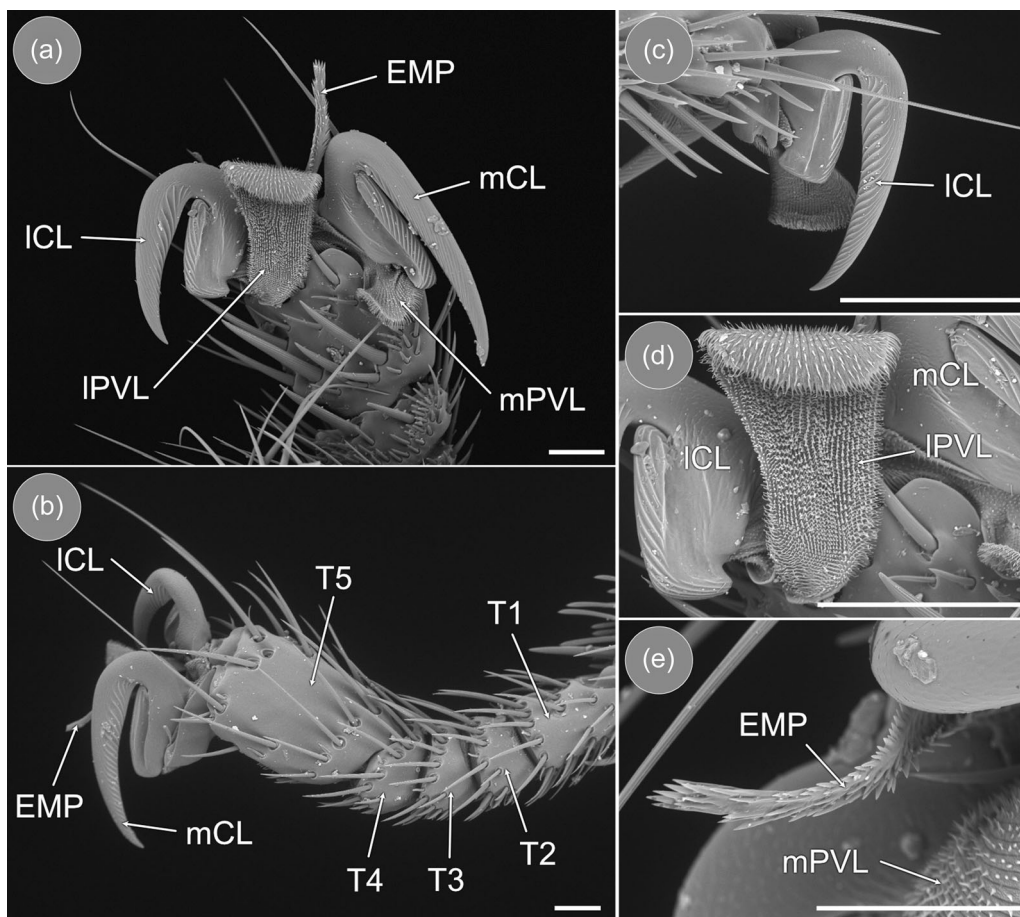


FIGURE 1 *Hippobosca equina*, scanning electron micrographs of the attachment system. (a) Ventral overview of the front leg: the asymmetry between the lateral and medial claws and pulvilli is clearly visible, the empodium is situated between the claws; scale = 100 μm . (b) Dorsal view of the hind leg with the five tarsomeres; scale = 100 μm . (c) Detailed view of the lateral monodentate claw with characteristic grooves on the outer side; scale = 300 μm . (d) Detailed ventral view of one pulvillus; scale = 200 μm . (e) Detailed ventral view of the empodium; scale = 100 μm . EMP, empodium; ICL, lateral claw; IPVL, lateral pulvillus; mCL, medial claw; mPVL, medial pulvillus; T1–T5 tarsomeres 1–5.

claws' tip (Figure 1a-c). The grooves on both sides of the claw meet proximally and form a sharp edge.

Similar to the claws, both pulvilli (PVL) differ in size as well (Figure 1a). The larger, lateral pulvillus (IPVL) is paired with the lateral, smaller claw. The pulvillus is broader distally while the last 60 μm of its distal tip bends proximally, covering the ventral side of the pulvillus (Figure 1a,d). IPVL is $328 \pm 26.5 \mu\text{m}$ long ($n = 2$) and has a width of $181.6 \pm 2.6 \mu\text{m}$ ($n = 2$) at its broadest part. At the point of emergence, it is $62.2 \pm 1.6 \mu\text{m}$ ($n = 2$) wide. Compared to this larger pulvillus, the medial pulvillus (mPVL) on the side of the medial, larger claw is small and almost roundly shaped (Figure 1a). mPVL is $98 \pm 6.4 \mu\text{m}$ long ($n = 2$) and has a width of $105.0 \pm 12.5 \mu\text{m}$ ($n = 2$) at its broadest part (Figure 1a).

The ventral and dorsal sides of the pulvilli are covered with acanthae (Figure 1a,d). The acanthae are arranged in rows from proximal to distal. The acanthae on the ventral side of the pulvilli show mostly a spatulate tip shape and are in total $23.8 \pm 3.2 \mu\text{m}$ ($n = 4$) long, while the spatulae tip is $4.1 \pm 0.7 \mu\text{m}$ ($n = 4$) long. The two second most lateral rows of acanthae consist of thicker acanthae without spatulate tip. The density of acanthae on IPVL is 7.0 ± 0.7 per $100 \mu\text{m}^2$ ($n = 4$), with a higher density of acanthae closer to the edges than in the middle of the pulvillus (Figure 1a,d). On the dorsal side of the pulvilli, $20.1 \pm 4.6 \mu\text{m}$ ($n = 4$) long acanthae could be found. Similar to those on the ventral side, these acanthae are organized in rows, but do not have a spatulate tip.

The empodium (EMP) of *H. equina*, emerging between the claws, is cylindrically shaped (Figure 1a,e). It is $264 \pm 3.5 \mu\text{m}$ long ($n = 2$) and $18.3 \pm 5.7 \mu\text{m}$ ($n = 4$) broad. The lateral sides as well as the ventral side of the empodium are covered with acanthae. The distal end of the empodium is lined with five spiny acanthae having a length of $14.4 \pm 1.6 \mu\text{m}$ ($n = 4$). Those spiny acanthae are also found on the lateral sides, but are slightly shorter at $10.2 \pm 1.7 \mu\text{m}$ ($n = 4$) in length (Figure 1e).

The lengths of the tarsus and tarsomeres are measured on the hind leg. The tarsus of *H. equina* is in total $987 \pm 54.7 \mu\text{m}$ ($n = 4$) long (Figure 1b). The first tarsomere (T1) is $284 \pm 10.4 \mu\text{m}$ ($n = 4$) long, the second tarsomere (T2)— $108.3 \pm 30.7 \mu\text{m}$ ($n = 4$), the third tarsomere (T3)— $112.7 \pm 32.9 \mu\text{m}$ ($n = 4$), the fourth tarsomere (T4)— $100 \pm 64.8 \mu\text{m}$ ($n = 4$), and the fifth tarsomere (T5) with $371 \pm 65.2 \mu\text{m}$ ($n = 4$) is the longest one. The legs and tarsi are covered with setae: Dorsally on the first four tarsomeres, lines of setae before the distal end of the segments are found, which also cover the lateral sides. These setae are $138 \pm 7.35 \mu\text{m}$ long ($n = 4$). A similar arrangement of setae is found on T5, starting 60 μm after its proximal edge (Figure 1b). These setae are up to $286.1 \pm 71.2 \mu\text{m}$ ($n = 4$) long. Additionally, T1 shows more setae besides those on the distal edge and also T5 has long setae distally with a length of 350–400 μm (Figure 1b). All tarsomeres are ventrally covered with shorter setae with a length of $19.4 \pm 4.0 \mu\text{m}$ ($n = 4$). Ventrally on T1 to T4, two spine-like setae are present, while T5 is covered with more of those thicker setae. Of these spine-like setae, two are especially thick with a diameter of $26.6 \pm 0.9 \mu\text{m}$ ($n = 4$) and a length of $197.1 \pm 10.7 \mu\text{m}$ ($n = 2$; Figure 1b).

The two monodentate claws of *L. cervi* have a similar shape, but differ in size (Figure 2). Both claws are ventrally curved and terminate by a pointed tip. The median claw (mCL) is larger than the lateral claw (ICL; Figure 2a). The larger mCL is $216 \pm 8 \mu\text{m}$ long ($n = 2$), while the smaller ICL measures $178 \pm 5.4 \mu\text{m}$ ($n = 2$) in length. The length of the larger claw base is $95 \pm 2.2 \mu\text{m}$ ($n = 2$), while that of the smaller claw is $57 \pm 1.8 \mu\text{m}$ ($n = 2$). Although differing in length, the claw tips do not differ much. The larger claw tip has a diameter of $0.97 \pm 0.2 \mu\text{m}$ ($n = 2$), while the smaller claw has a tip diameter of $0.89 \pm 0.13 \mu\text{m}$ ($n = 2$). The average size of the gap created by the curvature of the claw between claw and claw base is $28.5 \pm 1.5 \mu\text{m}$ ($n = 2$) and $30.25 \pm 1.48 \mu\text{m}$ ($n = 4$) for the larger and smaller claw, respectively. The maximum gap width between the claw tip and the base of the larger claw is $42.5 \pm 2.5 \mu\text{m}$ ($n = 2$) and for the smaller claw $35.25 \pm 2.59 \mu\text{m}$ ($n = 4$).

The medial sides of both claws are flattened, while the lateral sides are curved convex while running to the claws tip (Figure 2a,c). The few grooves on the claw are small, occurring both on the medial and lateral sides of each claw and meets at the proximal edge of the claw, where a sharp ridge is formed (Figure 2a,d). The flat, distal edge of the claw near the claws' base is elevated and formed like an anvil (Figure 2a,c,d). This anvil-like structure is $5.4 \pm 0.5 \mu\text{m}$ ($n = 4$) in height, $14 \pm 2.5 \mu\text{m}$ ($n = 4$) broad at the ventral side, and $4.7 \pm 2.0 \mu\text{m}$ ($n = 4$) broad at the dorsal side. The surface of this structure is covered with prominent grooves running diagonally from the dorsal to lateral side, further to the ventral and finally to medial side (Figure 2a).

The pulvilli (PVL), similar to the claws, have different sizes and shapes (Figure 2a,c). The larger pulvillus (IPVL) is sided with the smaller claw and the smaller pulvillus (mPVL) close to the larger claw. IPVL is $252.9 \pm 6.4 \mu\text{m}$ ($n = 4$) long and $52.2 \pm 10.8 \mu\text{m}$ ($n = 4$) broad and turns slightly broader apically. mPVL is only $34.8 \pm 3.6 \mu\text{m}$ long and $25.6 \pm 5.7 \mu\text{m}$ ($n = 4$) broad. Interestingly, both pulvilli possess ten parallel rows of tenent acanthae (Figure 2e). These tenent acanthae have $9.1 \pm 0.82 \mu\text{m}$ ($n = 4$) long shaft and a $2.3 \pm 0.3 \mu\text{m}$ ($n = 4$) long spatula. The spatula has a maximum width of 2 μm and are bent toward the distal end of the pulvilli. The density of spatulae on the pulvilli is 13.25 ± 1.29 ($n = 4$) per $100 \mu\text{m}^2$. The basis of acanthae has an oval shape (approx. $4 \times 3 \mu\text{m}^2$; Figure 2d).

The empodium (EMP) emerges between the pulvilli (Figure 2a-c,f). The empodium has the shape of a thick spine and is $110 \pm 2.5 \mu\text{m}$ ($n = 2$) long. The dorsal side of the empodium is not covered by setae or acanthae (Figure 2f). Similar to the empodium of *H. equina*, the empodium ends with small acanthae. The ventral and lateral sides are covered with bristle-like acanthae (Figure 2a). The open space between each of these acanthae is $5.1 \pm 1.6 \mu\text{m}$ ($n = 4$).

The tarsus of the front leg is only $386 \pm 17.5 \mu\text{m}$ ($n = 2$) long (Figure 2b,c). The tarsus consists of five tarsomeres. The first tarsomere (T1) is $57.5 \pm 42.59 \mu\text{m}$ ($n = 4$), the second tarsomere (T2)— $30 \pm 6.1 \mu\text{m}$ ($n = 4$), the third one (T3)— $33.2 \pm 12.2 \mu\text{m}$ ($n = 4$), the fourth one (T4)— $40.6 \pm 27.9 \mu\text{m}$ ($n = 4$), and the fifth tarsomere (T5)— $206.1 \pm 28.4 \mu\text{m}$ ($n = 4$) long. The first four tarsomeres bear a ring of setae around their distal edge, which surrounds the entire tarsomere

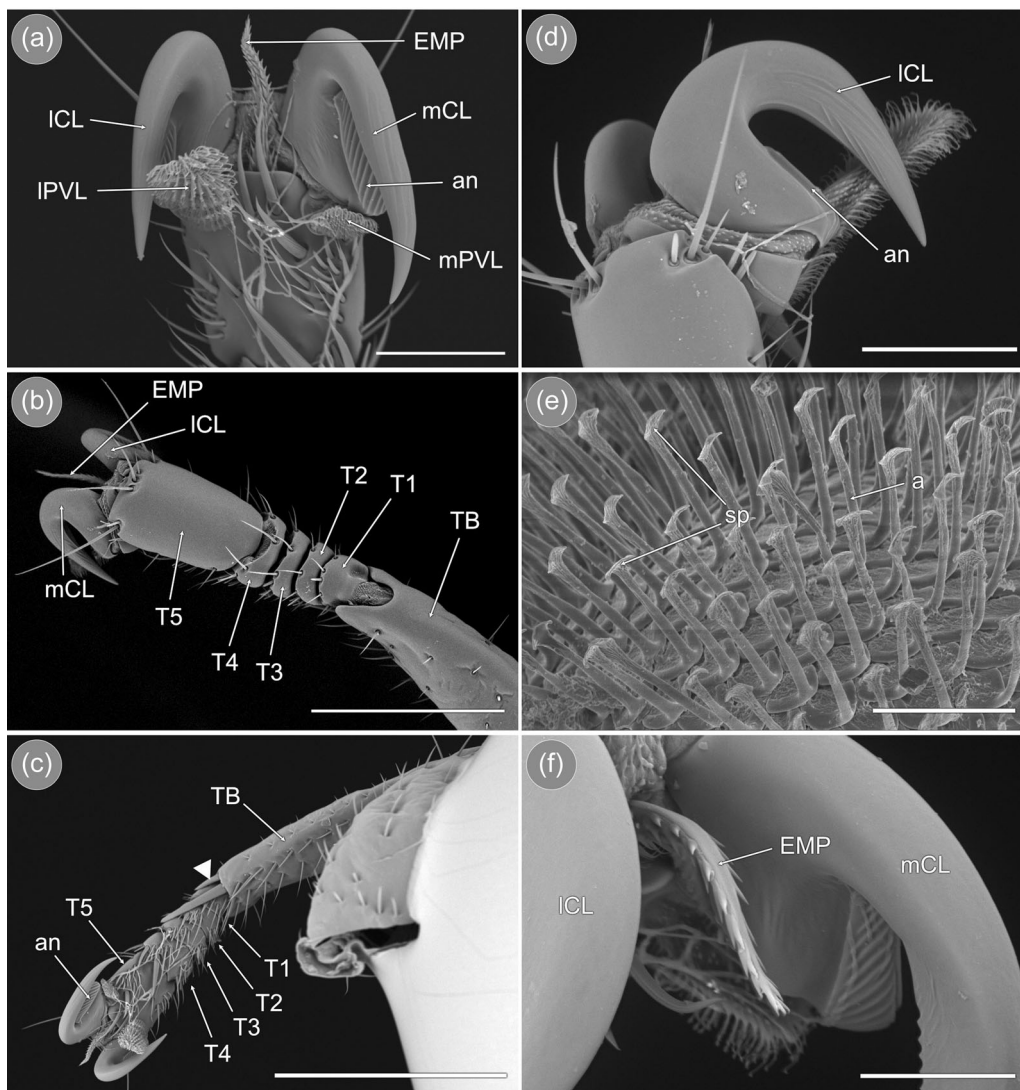


FIGURE 2 *Lipoptena cervi*, scanning electron micrographs of the attachment system. (a) Ventral overview of the mid leg: the asymmetry between the lateral and medial claws and pulvilli is clearly visible, the empodium is located between the claws; scale = 100 μm . (b) Dorsal overview of the front leg with five tarsomeres; scale = 300 μm . (d) Detailed view of the lateral monodentate claw with characteristic grooves on the outer side; scale = 100 μm . (e) Detailed view of the acanthae on the pulvillus; scale = 10 μm . (f) Detailed ventral view of the empodium; scale = 50 μm . a, acanthae; an, anvil; EMP, empodium; ICL, lateral claw; IPVL, lateral pulvillus; mCL, medial claw; mPVL, medial pulvillus; sp, spatulae; TB, tibia; T1–T5, tarsomeres 1–5.

except for a small spot in the middle of the ventral side of tarsomeres T2–T4. On the ventral side of the tarsomeres, the setae grow thicker. On T4, a thick bristle with a diameter of $12.5 \pm 1.4 \mu\text{m}$ ($n = 4$) and a length of $96.2 \pm 0.4 \mu\text{m}$ ($n = 2$) emerges (Figure 2c). Also, two stout bristles originate from the distal tibia: the first with a length of $159.7 \pm 0.6 \mu\text{m}$ ($n = 2$) and a diameter of $21.4 \pm 1.7 \mu\text{m}$ ($n = 4$) and the second one with a length of $62.3 \pm 1.0 \mu\text{m}$ ($n = 2$) and a diameter of $13 \pm 1.2 \mu\text{m}$ ($n = 4$) (Figure 2c). These two bristles end in direct contact with T1 (the smaller bristle) and T2 and T3, respectively (the longer bristle). On the ventro-distal end of T5, three setae with the length of $72.4 \pm 16.7 \mu\text{m}$ ($n = 4$) are present. Dorso-laterally of the distal end of T5, two $151.6 \pm 0.2 \mu\text{m}$ ($n = 2$) long setae originate, which surpass the length of the claws (Figure 2b,c).

3.3 | CLSM analyses of the attachment system of hippoboscid species

The CLSM maximum intensity projection of the autofluorescence signals of an entire tarsus indicated a heterogeneous material composition of the tarsal and pretarsal cuticle.

Generally, the tarsomeres of both *H. equina* and *L. cervi* are mostly chitin-dominated, which is indicated by the green and yellow autofluorescence signal (Figure 3). Only in *H. equina* do the tarsomeres appear to be more sclerotized laterally, as indicated by the yellow-orange color (Figure 3a,b). The joint regions, between the tarsomeres, as well as the centers of the tarsomeres are dominated by resilin (Figure 3). The fifth tarsomere of *L. cervi* is mainly composed of chitin with a

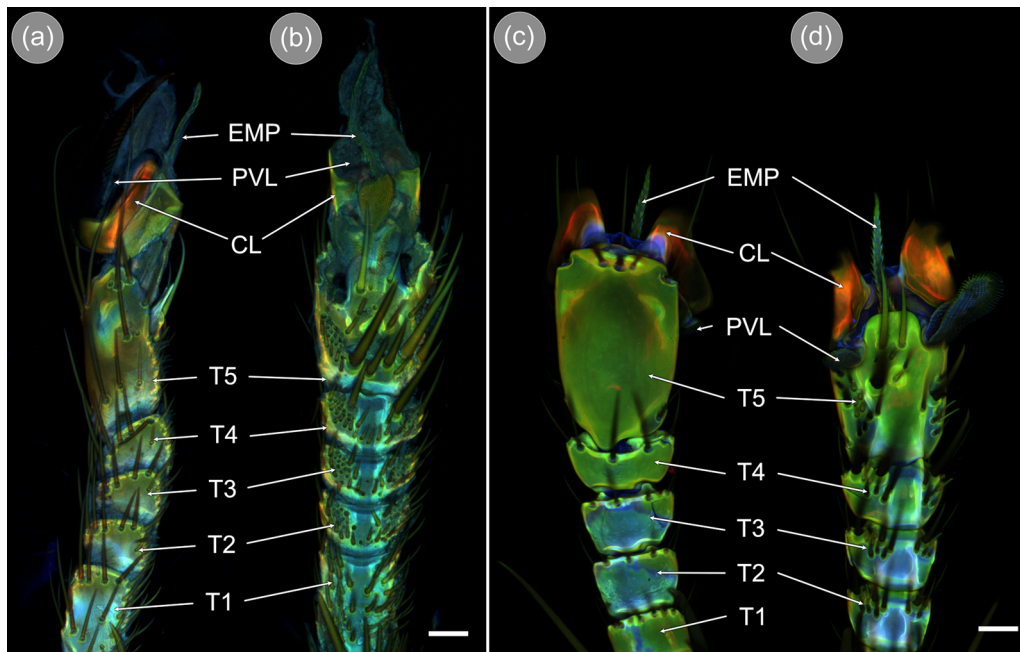


FIGURE 3 Confocal laser scanning microscopy (CLSM) images of the attachment system of *Hippobosca equina* and *Lipoptena cervi*. (a) Lateral view of the tarsus of *H. equina*, dorsal side on the left: the claws are only visible at the base; scale = 100 μm . (b) Ventral overview of a tarsus of *H. equina*, scale = 100 μm . (c) Dorsal view of the tarsus of *L. cervi*, scale = 50 μm . (d) Ventral view of the tarsus of *L. cervi*, scale = 50 μm . CL, claw; EMP, empodium; PVL, pulvillus; T1–T5, tarsomeres 1–5.

sclerotized triangular outline on the dorsal side, while the ventral lateral margins are softened by a cuticle supplemented with resilin (Figure 3c,d). The fifth tarsomere of *H. equina* is dorsally and laterally strongly sclerotized at the base and center of the tarsomere, with resilin-dominated patches in the lateral center of the tarsomere (Figure 3a). Ventrally, two resilin-dominated patches at the base and in the center are surrounded by chitin-dominated regions and sclerotized areas, while the distal top of the tarsomere contains high proportions of resilin (Figure 3b). The bases of the claws are sclerotized, indicated by the red autofluorescence (Figure 3a,b). The claws themselves as well as the pulvilli show no autofluorescence and appeared black in the CLSM maximum intensity projection (Figure 3a,b). The empodium of *H. equina* is both chitin- and resilin-supplemented (Figure 3a,b). In *L. cervi*, the bases of the claws are resilin-dominated at the very base, which can be clearly seen by the characteristic blue autofluorescence (Figure 3c). Followed by the resilin-containing joint region, the bases of the claws are heavily sclerotized (Figure 3c,d). The claws themselves show again no autofluorescence (Figure 3c,d). The pulvilli show weak autofluorescence in blue and green distally, indicating a soft and flexible material composition. The empodium is resilin-supplemented at the base and becomes more chitinous distally (Figure 3c,d).

3.4 | Morphology of the attachment system of the nycteribiid species

The tarsus of *B. nana* is equipped with two claws and two pulvilli, but no empodium (Figure 4a,b). The monodentate claws are thin, pointy,

and slightly curved toward the tarsus. The claws are $127 \pm 12.4 \mu\text{m}$ ($n = 2$) long with a diameter of $0.975 \pm 0.045 \mu\text{m}$ ($n = 2$). The big claw base is $72.8 \pm 0.8 \mu\text{m}$ ($n = 4$) long and the width ranged from $14.3 \pm 5.7 \mu\text{m}$ ($n = 4$) at the most proximal part to $36.8 \pm 5.2 \mu\text{m}$ ($n = 4$) at the distal part, where the claw emerges. The gap between claw base and claw is $12.33 \pm 1.25 \mu\text{m}$ ($n = 3$) wide at its proximal end and $20 \pm 1.41 \mu\text{m}$ ($n = 3$) at the distal end near the claws base (Figure 4a–c).

Grooves are present on both the claw itself and claw base (Figure 4a,c). On the claws, small grooves cover the proximo-lateral area, which run in parallel from the dorso-distal to the ventro-proximal direction almost all the way toward the claws tip (Figure 4c). Distally of the small grooves, two long and prominent grooves with a length of about $68.5 \pm 1.7 \mu\text{m}$ ($n = 4$) are found, covering almost 75% of the claw surface (Figure 4a). On the claw basis, many short but prominent grooves run parallel to the gap between the claw basis and claw itself. Only the part of the claw basis that faces the claw is covered with similar grooves that are found on the claws themselves. These narrow grooves run diagonally from dorso-distal to ventro-proximal (Figure 4c). The first dorsal $26.5 \pm 0.1 \mu\text{m}$ ($n = 2$) of the grooved claw base forms a thin edge that turns broader toward the ventral end (Figure 4b).

Similar to the claws, both pulvilli (PVL) of *B. nana* have the same size: no asymmetry between left and right pulvilli (and claws) is found (Figure 4a). The pulvilli measure $96 \pm 2.8 \mu\text{m}$ ($n = 2$) in length and emerge thin at the base, then turning slightly broader to $11.4 \pm 1.9 \mu\text{m}$ ($n = 4$) apically. Dorsally, the pulvilli are covered by small conical protuberances. Ventrally as well as laterally, acanthae

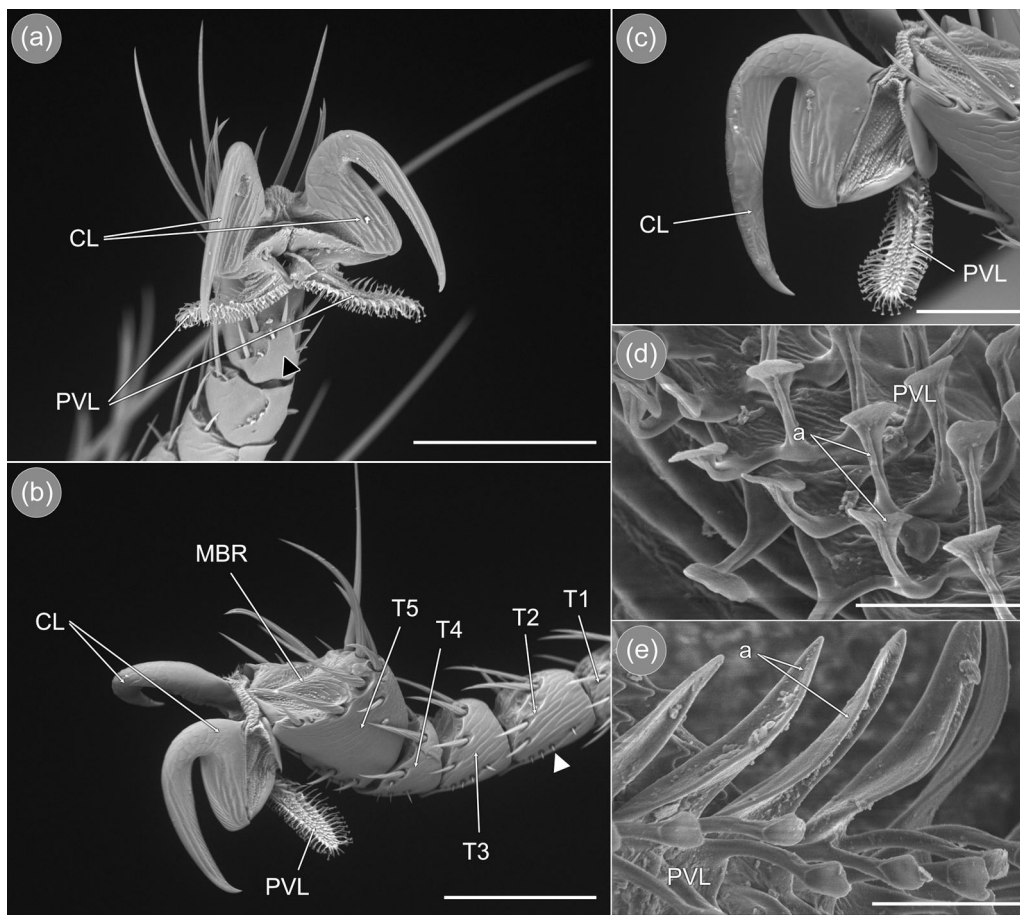


FIGURE 4 *Basilia nana*, scanning electron micrographs of the attachment system. (a) Ventral view of the tarsus, black triangle points at the cuneate structures; scale = 100 μm . (b) Dorsal view of the tarsus with the five tarsomeres, white triangle points at the short setae; scale = 100 μm . (c) Detailed view of the lateral monodentate claw with characteristic grooves on the outer side; scale = 50 μm . (d) Detailed view of the setae on the ventral pulvillus; scale = 5 μm . (e) Detailed view of setae on the lateral edge of the pulvillus; scale = 5 μm . a, acanthae; CL, claw; MBR, membranous structure; PVL, pulvillus; T1–T5, tarsomere 1–5.

with spatulated tips are present in rows at the pulvilli (Figure 4d,e). These acanthae have a $2 \pm 0.3 \mu\text{m}$ ($n = 3$) long shaft and a $1.5 \pm 0.2 \mu\text{m}$ ($n = 2$) long and $1.6 \pm 0.3 \mu\text{m}$ ($n = 3$) broad spatula (Figure 4d). The density of acanthae on the pulvilli is 13.25 ± 0.43 ($n = 4$) per $100 \mu\text{m}^2$. The most lateral row of acanthae has a different shape than the spatulated acanthae: with a length of $8.97 \pm 0.82 \mu\text{m}$ ($n = 4$), they are double the size of the spatulae and have a semicircular shape, which forms a small groove faced toward the ventral side of the pulvilli (Figure 4e). As mentioned above, *B. nana* does not possess an empodium.

The complete tarsus of the mid leg of *B. nana* is $748 \pm 21 \mu\text{m}$ ($n = 2$) long and consists of five tarsomeres (Figure 4b). The most prominent structure is the first tarsomere (T1) with a length of $490.1 \pm 18.0 \mu\text{m}$ ($n = 4$), making out 66.8% of the total length of the tarsus, while only being $45.1 \pm 4.6 \mu\text{m}$ ($n = 4$) broad (Figure 5a). The second tarsomere (T2) is $45.6 \pm 2.4 \mu\text{m}$ ($n = 4$) long, the third (T3) is $37.3 \pm 9.2 \mu\text{m}$ ($n = 4$), the fourth (T4) is $33.5 \pm 13.5 \mu\text{m}$ ($n = 4$), and the fifth tarsomere (T5) measures $98.3 \pm 28.4 \mu\text{m}$ ($n = 4$) in length (Figure 4b). These lengths are measured on its ventral side. Dorsally, T3 and T4 are shorter, giving these two tarsomeres a triangular shape

when viewed laterally. The T1 is tilted at 64° toward the tibia. Because of the stacked triangular tarsomeres, T5 is bent dorsally giving the impression that it is placed on top of the T4.

All five tarsomeres show a ring of setae surrounding their distal end. Laterally of T2–T5, three short setae are present (Figure 4b). In case of T2 to T4, these setae are only $6.8 \pm 0.5 \mu\text{m}$ ($n = 4$) long, while they are $30.0 \pm 0.5 \mu\text{m}$ ($n = 2$) long on T5. Ventrally of all tarsomeres, cuneate structures are found with their tips pointing distally (Figure 4a). On T2 and T3, these cuneate structures protrude over the distal end of the tarsomeres and overlap with the next segment for $6.6 \pm 0.3 \mu\text{m}$ ($n = 2$). On T5, this cuneate structure is bordered by two rows of setae. Dorsally, a membranous structure (MBR) is present at the distal end of T5, which is surrounded by setae (Figure 4b,c). This membranous structure has an oval shape and a protruding centerfold, while the lateral sides of the MBR are recessed into the distal end of T5 (Figure 4b).

Similar to *B. nana*, the claws of *N. kolenatii* are both of equal size with a length of $96 \pm 3.6 \mu\text{m}$ ($n = 2$) (Figure 5a–c). The claw base is $79.4 \pm 1.0 \mu\text{m}$ ($n = 4$) long. The socket, where the claw emerges from the claw base, is $20.9 \pm 0.8 \mu\text{m}$ ($n = 4$) thick. The pointy tip of the claw

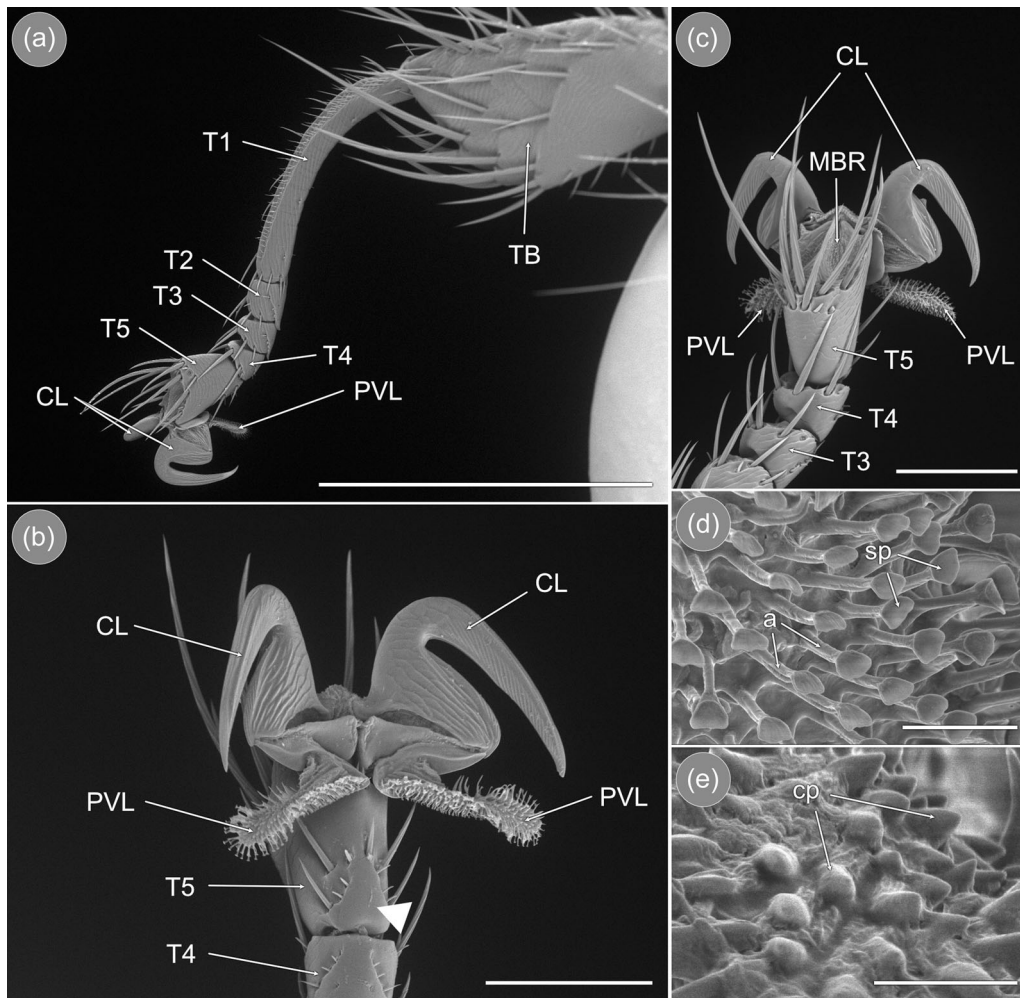


FIGURE 5 *Nycteribia kolenatii*, scanning electron micrographs of the attachment system. (a) Lateral view of the mid leg tarsus with the five tarsomeres and part of the tibia; scale = 500 μm . (b) Ventral view of the front leg tarsus, white triangle points at the triangular outgrowth; scale = 100 μm . (c) Dorsal view of the tarsus of the front leg; scale = 200 μm . (d) Detailed view of the acanthae on the ventral pulvillus; scale = 5 μm . (e) Detailed view of conical protrusions on the dorsal side of the pulvillus; scale = 5 μm . a, acanthae; CL, claw; cp, conical protrusions; MBR, membranous structure; PVL, pulvillus; sp, spatulae; TB, tibia; T1–T5, tarsomeres 1–5.

is bent toward the claw basis and has a diameter of $1.30 \pm 0.44 \mu\text{m}$ ($n = 2$). The average width of the claw gap is $11 \pm 0.82 \mu\text{m}$ ($n = 3$); the maximum width of $18.67 \pm 1.25 \mu\text{m}$ ($n = 3$). A similar pattern of grooves as on the claws of *B. nana* is present. Ventrally as well as dorsally, the proximal half of each claw facing the tarsomeres is covered with small grooves running from dorso-distal to ventro-proximal (Figure 5b,c). The distal edge of the claws from the base to the tip is not rounded, but rather forms a furrow between two protruding edges (Figure 5b,c). This furrow is $76.6 \pm 0.1 \mu\text{m}$ ($n = 2$) long and ends distally, when the two surrounding protrusions meet and form a blunt edge that runs toward the tip (Figure 5b). The claw base is laterally wide and flat on the dorsal edge and narrows down ventrally forming almost a protruding triangle (Figure 5c). Distally of this protruding triangle toward the proximal edge of the claw, a thinner outfold is formed covered with grooves. These distal grooves are mostly running parallel to the claw as well (Figure 5c). The fold is thinner and sharper at the dorsal edge of the claw base, while it becomes broader

and blunter ventrally toward the claw tip. The broader part of the fold opposing the proximal end of the claw is also covered with thin grooves that resemble chevrons pointing to the bending area of the claw (Figure 5b,c). Medially, the claw base is also covered with irregular grooves, which become more prominent ventrally (Figure 5b).

The pulvilli (PVL) of *N. kolenatii* are $94.8 \pm 2.4 \mu\text{m}$ ($n = 2$) long and $17.7 \pm 1.6 \mu\text{m}$ ($n = 4$) at its broadest (Figure 5b,c). Ventrally, the pulvilli are covered with spatulate acanthae (Figure 5b–d). These spatulae are $3.2 \pm 0.2 \mu\text{m}$ ($n = 4$) long and have a $1.70 \pm 0.13 \mu\text{m}$ ($n = 4$) long and broad head (Figure 5d). Dorsally, the pulvilli are covered with conical protuberances similar to those observed on *B. nana*'s pulvilli (Figure 5b,e). These conical structures have a diameter of $1.64 \pm 0.05 \mu\text{m}$ ($n = 4$) (Figure 5e). The acanthae surrounding them possess two heads (Figure 5b): one spatula-like similar to the spatulae on the ventral side and the other has a pointy end that emerges slanted from the shaft shortly before the spatulated tip. The density of acanthae on a pulvillus is 13.25 ± 1.30 per $100 \mu\text{m}^2$.

The tarsus and overall shape of the leg of *N. kolenatii* is similar to the morphology of *B. nana* (Figure 5). The distal end of the broad tibia (TB) of *N. kolenatii* is covered heavily with bristly setae (Figure 5a). The entire tarsus is $657 \pm 12.2 \mu\text{m}$ ($n = 2$) long, consisting of five tarsomeres. The first tarsomere (T1) is $358.1 \pm 20.2 \mu\text{m}$ ($n = 4$) long, which is 59.7% of the length of the entire tarsus (Figure 5a). The T1 is bent 90° ventrally. The second tarsomere (T2) is $56.0 \pm 1.6 \mu\text{m}$ ($n = 4$) long, the third tarsomere (T3) is $41.6 \pm 7.4 \mu\text{m}$ ($n = 4$) long, the fourth (T4) measures $32.8 \pm 17.6 \mu\text{m}$ ($n = 4$), and the fifth tarsomere is $94.0 \pm 20.9 \mu\text{m}$ ($n = 4$) long. The tarsomeres T2–T4 are slightly curved upwards, so that the fifth tarsomere is positioned 90° dorsally pointing in the same direction as the tibia (Figure 5a). Ventrally, on the distal ends of the tarsomeres, triangular outgrowths are found, which protrude distally on both the second and third tarsomeres and overlap with the next tarsomere for about $12.3 \pm 2.4 \mu\text{m}$ ($n = 2$; Figure 5a,b). Just like in *B. nana*, a row of setae is present dorsally at the distal edges of the tarsomeres (Figure 5a,c). Ventrally, short setae surround the outline of the triangular structures (Figure 5b). A membranous structure (MBR), which is also found on the tarsus of *B. nana*, is present on T5 as well (Figure 5c). It covers the entire distal edge of T5, showing two indentations divided by a thin central protrusion of the membrane (Figure 5c).

3.5 | CLSM analyses of the attachment system of the nycteribiid species

The tarsomeres of *B. nana* and *N. kolenatii* are mostly chitin-dominated as shown by the green autofluorescence signal (Figure 6). In *B. nana*, the first tarsomere (T1) seems to be more

strongly sclerotized ventrally toward its distal end and to the level of setae (Figure 6a). Toward the base of T1, the chitin-based material composition predominates and is only interrupted by resilin-rich sites arranged in horizontal stripes, which is indicated by the blue autofluorescence (Figure 6a). The tarsomeres T2–T5 are more sclerotized ventrally, especially in the triangular outgrowths (Figure 6a). The highest proportion of sclerotization is found in the center of triangular outgrowths. The outgrowths are surrounded by chitin-dominated cuticle (Figure 6a). Only T5 showed resilin-dominated cuticle surrounding the triangular outgrowths (Figure 6a). The setae show no autofluorescence and appear black. The pulvilli are resilin-dominated (Figure 6a). The T5 predominately consists of chitin apart from the membranous region, where the claws and other pretarsus structures are inserted (Figure 6a). The claws themselves show weak autofluorescence, but are more chitin-dominated basally and sclerotized distally of the bending point (Figure 6a,b). Dorsally, the tarsomeres are more sclerotized at their bases and resilin-dominated around the setae (Figure 6b). The joints between the tarsomeres are dominated by more resilin (Figure 6b). The membranous structure at the distal end of T5 is also resilin-dominated apart from two small sclerotized patches laterally of the central protrusion at the most distal edge (Figure 6b).

The tarsus of *N. kolenatii* is similar to that of *B. nana*, but less sclerotized with only sclerotized parts basally of the triangular outgrowths and in the region situated more lateral of the tarsomeres (Figure 6c,d). Distally of T4 before T5, a sclerotized patch is found in the center of the tarsomere (Figure 6c). The joint regions are resilin-dominated (Figure 6d). The pulvilli as well as the claw bases are made of resilin-dominated cuticle as shown by the blue autofluorescence signal (Figure 6d). The setae show weak autofluorescence and

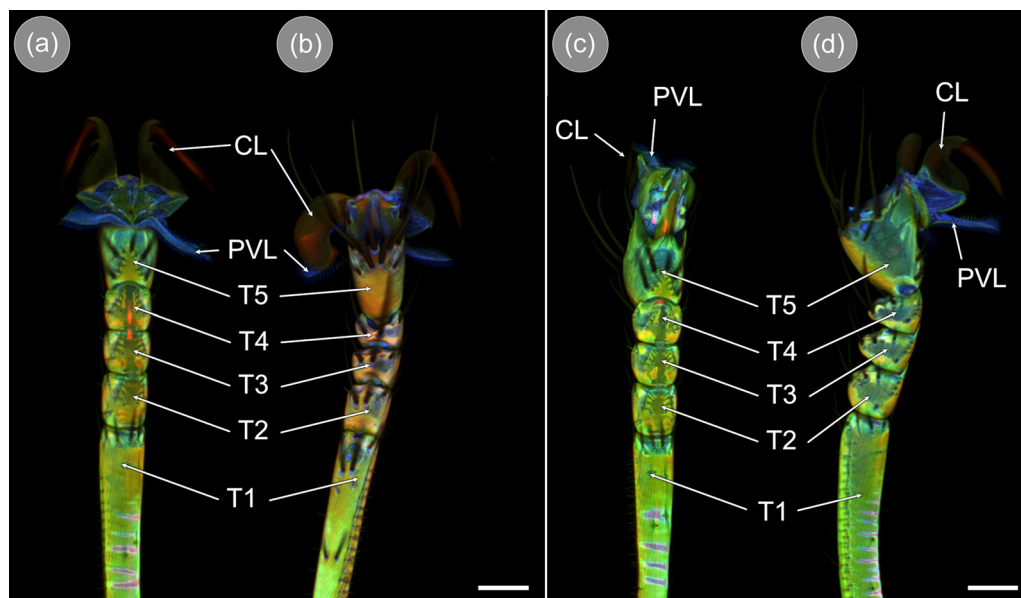


FIGURE 6 Confocal laser scanning microscopy (CLSM) images of the attachment system of *Basilia nana* and *Nycteribia kolenatii*. (a) Ventral view of a tarsus of *B. nana*; scale = $50 \mu\text{m}$. (b) Dorsal view of a tarsus of *B. nana*, scale = $50 \mu\text{m}$. (c) Ventral view of the tarsus of *N. kolenatii*, scale = $50 \mu\text{m}$. (d) Lateral view of the tarsus of *L. cervi*, scale = $50 \mu\text{m}$. CL, claw; PVL, pulvillus; T1–T5, tarsomeres 1–5.

appeared dark green, indicating a chitin-supplemented material composition (Figure 6c,d). As well as the setae, the claws show nearly no autofluorescence. The very base of the claws is sclerotized, becoming chitin-dominated at the bending point, before they become more sclerotized again toward the tip (Figure 6c,d).

4 | DISCUSSION

In the course of this study, the tarsal attachment systems of two hippoboscid and two nycteribiid dipteran species were investigated morphologically to find adaptations to their host surfaces. Generally, the attachment system of both hippoboscid species is similar. Both species have tarsi composed of five tarsomeres, while the most distal tarsomere bears a pretarsus with two monodentate claws of different sizes. The pulvilli are also asymmetrical, with the larger pulvillus situated on the side of the smaller claw. This result conforms with the findings of earlier studies on *H. equina* and *L. cervi* (Haarløv & Haarlov, 1964; J. I. Roberts, 1927).

However, some differences between the attachment systems could be identified. First, the sizes of the claws and pulvilli differ greatly being much larger in *H. equina* than in *L. cervi*. This is presumably due to their difference in body size, since *H. equina* measures about 12 mm from the head to abdomen tip and *L. cervi* is only about 7 mm long (Andreani et al., 2019; J. I. Roberts, 1927). Second, the tarsus of *H. equina* is also equipped with much more

setae than that of *L. cervi* (Figures 1 and 2). These setae are discussed as being mechanoreceptors (Andreani et al., 2019), but future studies will have to prove this assumption.

The asymmetry of the claws has a major advantage for life on hosts, since they form grasping gaps of two different sizes. This increases the possibilities of seizing hair of various diameters. The diameters of the coat hairs of *L. cervi*'s typical host, *Capreolus capreolus* (roe deer), vary between 100 and 250 μm (Meyer et al., 2001; Teerink, 2003; Supporting Information: Figure S1). *L. cervi* is mostly found at the anal and groin regions of the deer, where the fur is dense and covered by coat hairs (Haarløv & Haarlov, 1964). Since the coat hairs of *C. capreolus* are thicker than even the broadest gap between claw and claw base of *L. cervi* (42.5 μm), the ectoparasites seem not able to interlock with this type of hair. To move on thicker hairs, the parasites need to use a different attachment solution. Solitary coat hairs could be pushed against the fifth tarsomere by the claws and therefore captured by the pulvilli, which provide adhesion on more or less planar surfaces (S. N. Gorb, 2005; Büscher and Gorb, 2021; Figure 7b).

The pulvilli show, according to the CLSM results, an increase in sclerotization toward the tip as typical for other hairy insect attachment systems (Michels et al., 2016). Due to the different sizes of the pulvilli, morphological features of the attachment system appear to be functionally designed to adjust to the variance in the thickness of the hairs. Similar hypotheses have been established for *L. cervi* by J. I. Roberts (1927). When bringing two differently sized

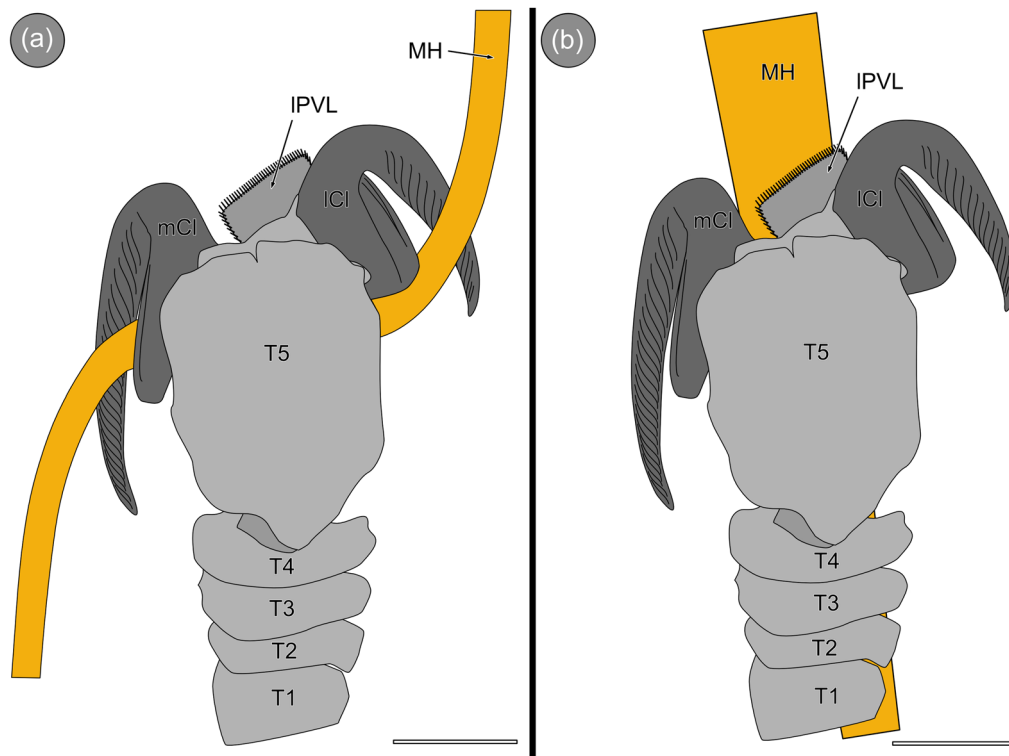


FIGURE 7 Schematic drawings of possible attachment solutions of Hippoboscidae. (a) Dorsal view of a tarsus clamping a thinner yellow hair by the claws gaps. (b) Dorsal view of a tarsus attaching to a thicker hair by the pulvillus. scale = 200 μm . ICL, lateral claw; mCL, medial claw; IPVL, lateral pulvillus; MH, mammal hair; T1–T5 = tarsomeres 1–5.

claws together to capture a hair, it leads to a changed positioning of the tarsus that is skewed toward the side with the smaller claw. Therefore, the side of the tarsus with the larger pulvillus is brought closer to the substrate and allows the larger pulvillus to attach, even though the tarsus is not placed horizontally on the substrate (J. I. Roberts, 1927). The woolen hairs of *C. capreolus*, however, are thinner than coat hairs (Teerink, 2003) and have an average width of 24.75 μm (Supporting Information: Figure S1). Thus, *L. cervi* can interlock with this type of hair using the claws and claw gaps, whose median width are 30.25 and 28.5 μm , respectively (see Figure 7a). This has also been previously observed by Haarlov and Haarlov (1964), who stated that *L. cervi* was attached to woolen hairs resulting in an almost perpendicular orientation of the parasite to the hosts' skin, being as close to the skin as possible.

The CLSM images of *L. cervi* show resilin-dominated claw bases with presumably a high resilience, low fatigue, and strong damping features (Michels et al., 2016). The high elasticity of the claw bases suggests that the claws can be moved relatively to the terminal tarsomere and possibly trap hairs of the host by both claws. It is also possible that the high elasticity at the claws base has a protective function so that the claws do not break off when anchored and too strong force is applied onto them. Distally to the resilin-dominated base, the claws are strongly sclerotized. This ensures their high stiffness and the claws are therefore able to manipulate the hairs of the host, for example, to anchor them in the region between the claw and claw base.

The situation in *H. equina* is similar. The coat hair diameter of horses varies and ranges between 60 and 90 μm (Supporting Information: Figure S1). Although the whole attachment system of *H. equina* is larger than that of *L. cervi*, the gap between claw and claw base is of a similar size with a maximum width of 29–53 μm . Therefore, *H. equina* seems also not to be able to interlock with the coat hair of horses. But *H. equina* is known to be not host specific and was found aside from horses on cattle, dogs, donkeys, bison, pigs, hares, birds, and humans (E. Austen, 1903; E. E. Austen, 1906; Becker & Bezzi, 1905; Grünberg, 1907; Nöller, 1914; Sokol & Michalski, 2015; Speiser, 1902, 1908). Apart from bird feathers, the hairs of these mammals are variously formed and have different diameters, all of which are thicker than the maximum gap width of the claws (Teerink, 2003). This list of observed host species and the investigated morphology of the attachment system of *H. equina* highlight again that the combination of asymmetric pulvilli and different-sized claws seems to enable an attachment to a variety of surfaces. Woolen hairs of horses, unlike these of roe deer, do differ in diameter from the coat hairs only moderately. They measure between 24 and 50 μm . Thus, woolen hairs of horses fit into the gap between the claw and claw base and allow an interlocking of *H. equina* with its host (Figure 7a). It has been observed that the gap between claw and claw base of *H. equina* forms an angle that is large enough to clasp thicker hairs, but sharp enough to exert a clamping effect (Hase, 1927). The ability to fit woolen hairs inside the claw gap could be the reason that *H. equina* is often found on areas, where woolen hairs or thinner hairs are present (Buxton, 1923; Sokol &

Michalski, 2015). By attaching to these sites, the parasites have easier access to the skin and are protected from the hosts' cleaning attempts (Haarlov & Haarlov, 1964). Additionally, this site selection presumably increases protection of the parasites from the wind and bad weather conditions and further allows them to use the host's body heat, since the woolen hairs are additionally covered by the coat hairs.

The CLSM images of *H. equina* reveal the differences of the attachment system to that of *L. cervi*. It is probably less sclerotized in general, with the biggest difference in the shape and material composition of the fifth tarsomere and pretarsus. The claws themselves appear most black in CLSM images, which might be due to a screening of the autofluorescence by the melanin embedded in the cuticle. The proximal part of the claws are only sclerotized laterally, but are chitin-dominated at the base. The larger asymmetrical pulvillus extend further distally and contains presumably large proportion of resilin. These structures could be potentially used as a clamp: both coat and woolen hairs could be clamped by both claws and additionally attached to the pulvilli. This way of attachment was hypothesized by J. I. Roberts (1927) and observed by Hase (1927) on *H. equina*. This attachment solution could be an adaptation to the flight ability, since *H. equina* is able to fly throughout its life and is not as dependent on its attachment system as *L. cervi* or as *Crataerina pallida* (Liu et al., 2019; D. S. Petersen et al., 2018). Additionally, the grooves on the claws of both studied hippoboscoid species could have an anisotropic friction effect, which enables a higher mechanical interlocking of the substrate hair by the claw gap. The empodium of both hippoboscoid species is resilin-dominated at the base and is getting more chitin-dominated toward the distal tip. Especially the bristles on the empodium are chitin-dominated, as shown in the CLSM scans. The CLSM is detecting the material distribution, but the precise material properties have to be studied by mechanical analyses.

The latest study on another hippoboscoid species, *Crataerina pallida*, argues that the empodium acts as a cleaning device (D. S. Petersen et al., 2018). The empodium of *C. pallida* is resilin-dominated at the base, but becomes chitin-dominated and further distally even sclerotized. The bristles on the empodium are longer and finer in *C. pallida*, but this could be an adaptation to clean the tridentate claws of *C. pallida*. If the empodia of both *H. equina* and *L. cervi* would also function as cleaning devices, it stands to reason that the bristles on their empodia are shorter, because their claws are monodentate and therefore coarser bristles are likely more appropriate to clean them.

In contrast to the differences of the attachment system in both representatives of Hippoboscidae studied here, the attachment system of the two nycteribiid species *B. nana* and *N. kolenatii* are similar. Both species have symmetrical tarsi with two monodentate claws, two similar-sized pulvilli, and no empodium. Claws and pulvilli of *B. nana* are the smallest of all attachment devices investigated here. *Basilina nana* is monoxenous for the bat *Myotis bechsteinii*, while *N. kolenatii* parasitizes the bat species *M. daubentonii*, although the latter has occasionally been found on other *Myotis* species

(Maa, 1969; Scheffler, 2010; Szentiványi et al., 2016). Since all Nycteribiidae are wingless, they are dependent on their attachment system to fulfill their life cycle.

Bats offer two surfaces for ectoparasites to live on: the fur and the wing membranes. It has been observed in tropical bats that species of the Nycteribiidae live in the fur and not on the almost hairless wing membranes (Ter Hofstede et al., 2004). Unlike the hairs of other mammals, hairs of bats show no differentiation between woolen hair and coat hair (Nason, 1948; Supporting Information: Figure S1). Hairs of most bats, among those species belonging to *Myotis*, are about 10 μm in diameter (Hausman, 1920; Teerink, 2003). Therefore, there is no difference of the fur between the host species of these bat flies. Morphological adaptations for the life in the fur of bats are long legs, especially the hind legs, and ctenidia, rows of stout setae on the thorax and abdomen that work as a comb (Ter Hofstede et al., 2004). The long legs are also present in *B. nana* and *N. kolenatii*.

The morphology of the legs and especially that of the first tarsomere of the two nycteribiid species diverges from that of the hippoboscids. This is most likely due to their adaptation to the bats as hosts. The ratio of the body size between the bat and bat flies is much smaller than in the other studied fly species. Therefore, the substrate of nycteribiid species is much more curved than the corresponding substrates of the Hippoboscidae, which makes it challenging for the bat flies to attach themselves to the rounded surfaces. We assume that the long legs and the curved first tarsomere allow them to adapt better to round substrates than if the legs would be shorter and less curved.

The fast movement of Nycteribiidae in the fur of their hosts is described as a movement similar to swimming (Marshall, 1982). Unlike the two hippoboscids parasitizing larger mammals, the two nycteribiid species are morphologically able to clamp all hairs of their hosts in the gap of their claw, since the width of the gap is between 11 and 20 μm wide, so slightly broader than that of the diameter of the host hair (Teerink, 2003). Due to the small diameter of the host hairs, the coronal scales on the hairs have a big impact on the hair surface structure leading to an alternating thickness along the length of the hair (Hausman, 1930; Teerink, 2003). The combination of heavily structured hairs and the claw gap that is only slightly broader than the hair diameter should lead to an effective attachment, once a single hair is caught into the gap. Since the claw gap is longer than broad, it is also possible to clamp more than one hair in the gap and increase interlocking, since the hairs with broad scales also may interact with each other and decrease the chance of slipping out of the claw gap. To get the hair in contact and to interlock with the claw, the tarsus has to be simply placed in the fur and pulled backwards while spreading the claws to get the most effective contact angle with the hair. Due to the coronal structure of the bat hairs, it is important on which location the hair and the claws interlock with each other. This tarsal position would potentially make sideways movement along the hairs possible. The CLSM scans of the bat fly tarsi indicate a high elasticity of the membrane connecting the fifth tarsomere and claws or pretarsus respectively. This elasticity likely allows for a high movability of the claws, which is also common

in nonparasitic flies and other insect taxa, which have been discussed as claw-returning string and passive stabilizer (S. N. Gorb, 1996; Niederegger et al., 2003). In Nycteribiidae, this high elasticity of the claws might especially be helpful for a firm attachment and for moving on substrates with a different curvature depending on the flies' position on the host.

Another possible way of attaching is the clamping of a hair by both claws when they get brought together, similarly to *H. equina* and *L. cervi*. If nycteribiid species use this way of attachment, it is probably only used for staying in place for a short time span, for example, during running.

Not only the size of the claw gap at its median, but also the width of pulvilli in both bat fly species is close to the hair diameter (10 μm) with 11 μm for *B. nana* and 16 μm for *N. kolenatii*. This allows them to attach to a single hair with their entire pulvillus if they are aligned, enabling contact of all spatulated acanthae with the hair. If the pulvillus is broader than the hair, the high elasticity of the pulvilli, indicated by the CLSM scans, might allow them to embrace the hair from more than one side. On the tarsi of both bat flies, the pulvilli are facing laterally away from the fifth tarsomere and are not positioned next to each other. If the fifth tarsomere is pressed ventrally on the substrate, the attachment of both pulvilli could lead to an increase in contact area and in turn to enhancement of attachment forces. The pulvilli could also potentially attach to the hairs that are caught in the claw gap to ensure even stronger attachment.

The density of acanthae was surprisingly similar between three of the four fly species studied. The smaller species have the higher density: *B. nana*, *N. kolenatii*, and *L. cervi* with 13.3 per 100 μm^2 . *H. equina* with 7.0/100 μm^2 had the lowest density of acanthae. The density of other calyptrate species is 14.0/100 μm^2 for *Calliphora calliphoroides* (Rohdendorf, 1931), 38.0/100 μm^2 for *Lucilia sericata* (Meigen, 1826) and 19.0/100 μm^2 for *Muscina stabulans* (Fallen, 1817) (D. S. Petersen et al., 2018; Wang et al., 2016). D. S. Petersen et al. (2018) measured the density of tenent acanthae of another hippoboscids fly *Crataerina pallida*, which was around 70.0/100 μm^2 . This means that ectoparasites that are stronger associated with their preferred substrates as free-living flies may not necessarily have higher density of acanthae on their pulvilli, which supports the idea that pulvilli play only a supplementary role in their attachment to the host.

In addition to Nycteribiidae, representatives of the family Streblidae are also known to parasitize bats (Dick et al., 2007). Many Streblidae keep their wings and are still able to fly (Brown et al., 2009). The morphology of different species in Streblidae is more divergent than that of Nycteribiidae, especially the shape of the thorax and length of the legs (Brown et al., 2009). Some species show similarities with the studied nycteribiid species: long legs, strong claws, and well-developed ctenidia (Brown et al., 2009). The wingless bat fly *Mystacinobia zelandica* (Diptera, Mystacinobiidae) is an endemic fly species that lives on the lesser short-tailed bat *Mystacina tuberculata* in New Zealand (Holloway, 1976). It feeds on the bats guano and is therefore not parasitic (Holloway, 1976). The morphology, especially of the legs of *M. zelandica*, resembles the

morphology of the two studied Nycteribiidae. The legs are elongated, the tarsus is slightly curved and possesses a long first tarsomere (Holloway, 1976). The tarsi of the species possess an empodium, two small pulvilli, and two claws that look similar to the claws of *B. nana* and *N. kolenatii* (Holloway, 1976). The similar shape of legs and claws of Nycteribiidae, Mystacinobiidae, and some Streblidae indicates that these long legs and the large claws are indeed an adaptation to their similar substrate, the pelage of their bat hosts.

However, there is no evidence of the attachment system of *B. nana* and *N. kolenatii* being evolutionary adapted specifically to their monoxenous host, except for the long hind legs implying an adaptation to the attachment on fur (Ter Hofstede et al., 2004). The dimensions of both the bat fur and attachment system of the bat flies are rather similar to each other. Former studies have already excluded that the host-specificity is based on ecological isolation; therefore, the host-specificity is down to the morphological specialization of the host itself (Ter Hofstede et al., 2004). Since the specialized adaptation to the host is not based on the tarsal attachment system, future studies should focus on other morphological structures directly interacting with the host, for example, the mouthparts. The monoxenous bat flies can live on any bat to survive on its blood, but for reproduction the blood of the genuine host is needed (Marshall, 1976, 1981; Wenzel et al., 1966). The evolutionary adaptation to the specific host is therefore likely to be found in the morphology of the mouthparts.

5 | CONCLUSIONS

In Hippoboscoidea, the claws seem to be the most important attachment structures, since they are used as hooks that attach to structures on the host surface. The claw tips seem less important than the gaps between the claws and the claw bases, when attaching to and moving on the hosts' fur.

H. equina and *L. cervi* use an approach with a simple claw morphology, since the substrates on their hosts are heterogeneous, consisting of thick coat hairs, thinner woolen hair, and areas without hairs. Similar to avian hippoboscoid species (D. S. Petersen et al., 2018), woolen hairs get caught in the gap between the claw base and claw. Another way of attachment to thicker hair is the use of the claws as a clamp, clasping hairs by the claws that were brought together. The species of the Nycteribiidae possess claws where the gap between these claws is of the same size as the hair diameter of the host species. Since the bats only possess homogeneous fur, hairs can get caught into the claw gap.

The pulvilli of hippoboscoid and nycteribiid species parasitizing larger mammals probably attach to only a single hair, since the hairs of their host species are often the same size or broader than the pulvilli. Thus, all spatulate acanthae are in contact with the surface of the same hair. Due to the large size of the host hairs, many acanthae can be in contact with the hair at a time, which ensures good contact formation with more basal spatulated tips. For the smaller woolen

hairs (which are present in horses or deer), only few of the tenent acanthae of the fly pulvillus are able to be in contact. Therefore, it is likely that the large pulvillus only gets in contact with the hair of the undercoat to prevent sliding along the interlocked claws and to keep them in contact with the claws. In Nycteribiidae, it is possible that they can get positioned to align perfectly with the hair and all acanthae of one pulvillus can attach to it.

AUTHOR CONTRIBUTIONS

Sarah Hayer: Writing – original draft; writing – review & editing; visualization. **Beeke P. Sturm:** Writing – original draft; writing – review & editing; Investigation. **Sebastian Büsse:** Conceptualization; supervision; writing – review & editing. **Thies H. Büscher:** Investigation; writing – review & editing. **Stanislav N. Gorb:** Conceptualization; writing – review & editing; project administration; supervision.

ACKNOWLEDGMENTS

The authors would like to thank Prof. Matthias Starck and Prof. Rolf Beutel for carefully reviewing the manuscript. We also would like to thank Dennis Petersen for his support during the project and data acquisition.

DATA AVAILABILITY STATEMENT

The data that support the findings of this study are available in the Supporting Information of this article.

ORCID

Sarah Hayer  <http://orcid.org/0000-0002-6804-6166>

Sebastian Büsse  <http://orcid.org/0000-0002-1657-7950>

REFERENCES

- Andreani, A., Sacchetti, P., & Belcari, A. (2019). Comparative morphology of the deer ked *Lipoptena fortisetosa* first recorded from Italy. *Medical and Veterinary Entomology*, 33(1), 140–153. <https://doi.org/10.1111/mve.12342>
- Austen, E. (1903). Notes on Hippoboscidae in the collections of the British museum. *Annals and Magazine of Natural History* 12(7), 255–266.
- Austen, E. E. (1906). *Illustrations of British blood-sucking flies*. Order of the Trustees of the British museum.
- Becker, T., & Bezzi, M. (1905). *Katalog der Paläarktischen Dipteren IV. Cyclorrhapha, Schizophora, Holometopa* (pp. 23–37).
- Bequaert, J. C. (1953). The Hippoboscidae or louse-flies (Diptera) of mammals and birds. Part I. Structure, physiology and natural history. *Entomologica Americana*, 33, 211–442.
- Brown, B. V., Borkent, A., Cumming, J. M., Wood, D. M., Woodley, N. E., & Zumbado, M. A. (2009). *Manual of Central American Diptera* (Vol. 1, p. 728). NRC Research Press.
- Büscher, T. H., & Gorb, S. N. (2021). Physical constraints lead to parallel evolution of micro-and nanostructures of animal adhesive pads: A review. *Beilstein Journal of Nanotechnology*, 12(1), 725–743.
- Büscher, T. H., Petersen, D. S., Bijma, N. N., Bäuml, F., Pirk, C. W. W., Büsse, S., Heepe, L., & Gorb, S. N. (2021). The exceptional attachment ability of the ectoparasitic bee louse *Braula coeca* (Diptera, Braulidae) on the honeybee. *Physiological Entomology*, 47, 83–95. <https://doi.org/10.1111/phen.12378>
- Büsse, S., & Gorb, S. N. (2018). Material composition of the mouthpart cuticle in a damselfly larva (Insecta: Odonata) and its biomechanical significance. *Royal Society Open Science*, 5(6), 172117.

- Buxton, P. A. (1923). Applied entomology of Palestine, being a report to the Palestine Government. *Bulletin of Entomol Research*, 14, 289–340.
- Combes, C. (2001). *Parasitism: The ecology and evolution of intimate interactions* (p. 552). University of Chicago Press.
- Dai, Z., Gorb, S. N., & Schwarz, U. (2002). Roughness-dependent friction force of the tarsal claw system in the beetle *Pachnoda marginata* (Coleoptera, Scarabaeidae). *Journal of Experimental Biology*, 205(16), 2479–2488.
- Dick, C., Patterson, B., & Dittmar, K. (2007). Bat flies: Obligate ectoparasites of bats (Mammalia: Chiroptera). *Bat Research News*, 48(3), 111–112.
- Friedemann, K., Schneeberg, K., & Beutel, R. G. (2014). Fly on the wall—attachment structures in lower Diptera. *Systematic Entomology*, 39(3), 460–473.
- Gorb, S., & Beutel, R. (2001). Evolution of locomotory attachment pads of hexapods. *Naturwissenschaften*, 88(12), 530–534. <https://doi.org/10.1007/s00114-001-0274-y>
- Gorb, S. N. (1996). Design of insect unguitractor apparatus. *Journal of Morphology*, 230(2), 219–230.
- Gorb, S. N. (2001). *Attachment devices of insect cuticle*. Springer Science & Business Media.
- Gorb, S. N. (2005). Uncovering insect stickiness: Structure and properties of hairy attachment devices. *American Entomologist*, 51(1), 31–35.
- Grünberg, K. (1907). *Die blutsaugenden Dipteren. Leitfaden zur allgemeinen Orientierung, mit besonderer Berücksichtigung der in den deutschen Kolonien lebenden Krankheitsüberträger*. Jena.
- Haarløv, N., & Haarløv, N. (1964). Life cycle and distribution pattern of *Lipoptena cervi* (L.) (Dipt., Hippobosc.) on Danish deer. *Oikos*, 15(1), 93–129.
- Hase, A. (1927). Beobachtungen über das Verhalten, den Herzschlag sowie den Stech- und Saugakt der Pferdelausfliege *Hippobosca equina* L. (Diptera, Pupipara) (diptera, pupipara). *Zeitschrift Für Morphologie Und Ökologie Der Tiere*, 8(1–2), 187–240.
- Hausman, L. A. (1920). Structural characteristics of the hair of mammals. *The American Naturalist*, 54(635), 496–523.
- Hausman, L. A. (1930). Recent studies of hair structure relationships. *The Scientific Monthly*, 30(3), 258–277.
- Ter Hofstede, H. M., Fenton, M. B., & Whitaker, J. O. Jr. (2004). Host and host-site specificity of bat flies (Diptera: Streblidae and Nycteribiidae) on neotropical bats (Chiroptera). *Canadian Journal of Zoology*, 82(4), 616–626. <https://doi.org/10.1139/z04-030>
- Holloway, B. A. (1976). A new bat-fly family from New Zealand (Diptera: Mystacinobiidae). *New Zealand Journal of Zoology*, 3(4), 279–301. <https://doi.org/10.1080/03014223.1976.9517919>
- Kaitala, A., Kortet, R., & Laaksonen, S. (2009). Deer Ked, an ectoparasite of moose in Finland: A brief review of its biology and invasion. *Alces: A Journal Devoted to the Biology and Management of Moose*, 45, 85–88–88.
- Kemper, H. (1951). Beobachtungen an *Crataerina pallida* Latr. und *Melophagus ovinus* L. (Diptera, Pupipara). *Zeitschrift für Hygiene (Zoologie)*, 39, 225–259.
- Liu, S.-P., Friedrich, F., Petersen, D. S., Büsse, S., Gorb, S. N., & Beutel, R. G. (2019). The thoracic anatomy of the swift lousefly *Crataerina pallida* (Diptera) - functional implications and character evolution in Hippoboscoidea. *Zoological Journal of the Linnean Society*, 185, 111–131. <https://doi.org/10.1093/zoolinnean/zly032>
- Lloyd, J. E. (2002). Louse flies, keds, and related flies (Hippoboscoidea). In Reimer, L., & Weeks, E. (Eds.), *Medical and veterinary entomology* (pp. 349–362). Academic Press.
- Maa, T. C. (1969). A revised checklist and concise host index of Hippoboscoidea (Diptera). *Pacific Insects Monograph*, 20, 261–299.
- Marshall, A. G. (1976). Host-specificity amongst arthropods ectoparasitic upon mammals and birds in the New Hebrides. *Ecological Entomology*, 1, 189–199.
- Marshall, A. G. (1981). *The ecology of ectoparasitic insects*. Academic Press.
- Marshall, A. G. (1982). Ecology of insects ectoparasitic on bats. In T. H. Kunz (Ed.), *Ecology of bats*. Springer. https://doi.org/10.1007/978-1-4613-3421-7_10
- Meyer, W., Pohlmeier, K., Schnapper, A., & Hülmann, G. (2001). Subgroup differentiation in the Cervidae by hair cuticle analysis. *Zeitschrift für Jagdwissenschaft*, 47(4), 253–258.
- Michels, J., Appel, E., & Gorb, S. N. (2016). Functional diversity of resilin in Arthropoda. *Beilstein Journal of Nanotechnology*, 7(1), 1241–1259. <https://doi.org/10.3762/bjnano.7.115>
- Michels, J., & Gorb, S. N. (2012). Detailed three-dimensional visualization of resilin in the exoskeleton of arthropods using confocal laser scanning microscopy. *Journal of Microscopy*, 245(1), 1–16. <https://doi.org/10.1111/j.1365-2818.2011.03523.x>
- Nason, E. S. (1948). Morphology of hair of eastern North American bats. *American Midland Naturalist*, 39(2), 345–361.
- Niederegger, S., & Gorb, S. (2003). Tarsal movements in flies during leg attachment and detachment on a smooth substrate. *Journal of Insect Physiology*, 49(6), 611–620. [https://doi.org/10.1016/S0022-1910\(03\)00048-9](https://doi.org/10.1016/S0022-1910(03)00048-9)
- Nöller, W. (1914). Die blutsaugenden Insekten als Krankheitsüberträger. *Monatshefte f. prakt. Tierheilk*, 25.
- Oldroyd, H. (1966). The wing of *Crataerina pallida* (Latreille) (Diptera: Mippoboscoidea). *Proceedings of the Royal Entomological Society of London. Series B, Taxonomy*, 35, 23–25.
- Persson, B. N. J., & Gorb, S. (2003). The effect of surface roughness on the adhesion of elastic plates with application to biological systems. *The Journal of Chemical Physics*, 119(21), 11437–11444.
- Petersen, D. S., Kreuter, N., Heepe, L., Büsse, S., Wellbrock, A. H. J., Witte, K., & Gorb, S. N. (2018). Holding tight on feathers—structural specializations and attachment properties of the avian ectoparasite *Crataerina pallida* (Diptera, Hippoboscoidea). *Journal of Experimental Biology*, 221(13), jeb179242. <https://doi.org/10.1242/jeb.179242>
- Petersen, F. T., Meier, R., Kutty, S. N., & Wiegmann, B. M. (2007). The phylogeny and evolution of host choice in the Hippoboscoidea (Diptera) as reconstructed using four molecular markers. *Molecular Phylogenetics and Evolution*, 45(1), 111–122.
- Pohl, H. (2010). A scanning electron microscopy specimen holder for viewing different angles of a single specimen. *Microscopy Research and Technique*, 73(12), 1073–1076.
- Reckardt, K., & Kerth, G. (2006). The reproductive success of the parasitic bat fly *Basilina nana* (Diptera: Nycteribiidae) is affected by the low roost fidelity of its host, the Bechstein's bat (*Myotis bechsteinii*). *Parasitology Research*, 98(3), 237–243.
- Richards, A. G., & Richards, P. A. (1979). The cuticular protuberances of insects. *International Journal of Insect Morphology and Embryology*, 8(3–4), 143–157.
- Roberts, J. I. (1927). The anatomy and morphology of *Hippobosca equina*. *Annals of Tropical Medicine & Parasitology*, 21(1), 11–26. <https://doi.org/10.1080/00034983.1927.11684514>
- Roberts, L. S., & Janovy, J. Jr. (2000). *Gerald D. Schmidt e Larry S. Roberts' foundations of parasitology* (p. xviii–670). McGraw-Hill.
- Scheffler, I. (2010). Ektoparasiten der Fledermäuse in Winterquartieren in Brandenburg. *Märkische Ent. Nachr.* 12(1), 119–132.
- Sokol, R., & Michalski, M. M. (2015). Occurrence of *Hippobosca equina* in Polish primitive horses during the grazing season. *Annals of Parasitology*, 61(2), 119–124.
- Speiser, P. (1902). Studien über Diptera Pupipara. *Zeitschr. f. system. Hymenopt. u. Diptero*. 2. Jg. Tesehendorf i. Meekl.
- Speiser, P. (1908). Die geographische Verbreitung der Diptera Pupipara und ihre Phylogenie. *Zeitschr. f. wiss. Insektenbiol* (p. 4).
- Szentiványi, T., Estók, P., & Földvári, M. (2016). Checklist of host associations of European bat flies (Diptera: Nycteribiidae, Streblidae). *Zootaxa*, 4205(2), 101–126.

- Teerink, B. J. (2003). *Hair of West European mammals: Atlas and identification key* (p. 236). Cambridge University Press.
- Walker, G., Yulf, A. B., & Ratcliffe, J. (1985). The adhesive organ of the blowfly, *Calliphora vomitoria*: A functional approach (Diptera: Calliphoridae). *Journal of Zoology*, 205(2), 297–307.
- Wang, Q. K., Yang, Y. Z., Li, X. Y., Li, K., & Zhang, D. (2016). Comparative ultrastructure of pretarsi in five calyptrate species. *Parasitology Research*, 115(6), 2213–2222. <https://doi.org/10.1007/s00436-016-4963-z>
- Wenzel, R. L., Tipton, V. J., & Kiewlicz, A. (1966). *The streblid batflies of Panama (Diptera Calyptratae: Streblidae)*. Field Museum of Natural History Chicago.
- Whitaker, J. O. Jr. (1988). *Collecting and preserving ectoparasites for ecological study*. Johns Hopkins University Press.

SUPPORTING INFORMATION

Additional supporting information can be found online in the Supporting Information section at the end of this article.

How to cite this article: Hayer, S., Sturm, B. P., Büsse, S., Büscher, T. H., & Gorb, S. N. (2022). Louse flies holding on mammals' hair: Comparative functional morphology of specialized attachment devices of ectoparasites (Diptera: Hippoboscoidea). *Journal of Morphology*, 283, 1561–1576. <https://doi.org/10.1002/jmor.21523>